Journal of Molecular Modeling (2018) 24: 181
https://doi.org/10.1007/s00894-018-3719-3

ORIGINAL PAPER

GIAO-DFT-NMR characterization of fullerene-cucurbituril complex: the effects of the C_{60}@CB[9] host-guest mutual interactions

Guilherme Colherinhas[1] · Eudes Eterno Fileti[2] · Thaciana Malaspina[2]

Received: 3 April 2018 / Accepted: 12 June 2018 / Published online: 29 June 2018

Abstract

Magnetic shielding constants for an isolated fullerene C_{60}, cucurbituril CB[9], and the host-guest complex C_{60}@CB[9] were calculated as a function of separation of the monomers. Our results in the gas phase and water indicate a significant variation of the magnetic properties for all atoms of the monomers in the complex and after liberation of fullerene C_{60} from the interior of the CB[9] cavity. The interaction between the two monomers results in a charge transfer that collaborates with a redistribution of electron density to deshield the monomers.

Keywords GIAO-DFT-NMR · C_{60} fullerene · Cucurbit[9]uril · Host-guest complex

Introduction

The study of magnetic shielding constants for organic compounds can be one of the most powerful properties to define how the electron density distributes in compounds, as well as their structural characteristics [1–3]. Recent studies show that the electron delocalization, mainly observed in electron π networks, has similarities with the constant behavior of magnetic shielding in the compound [4, 5]. In this sense, use of the magnetic spectroscopic property to study the interaction between compounds in host-guest complexes, which exhibit charge transitions, can theoretically elucidate specific behaviors and characteristics of a certain family of these complexes. The results obtained with such techniques can provide the expansion of use of the host-guest system especially in nanotechnology.

Several important developments involving host-guest complexes, such as cyclodextrins, calixarenes, and, more recently, cucurbiturils have been reported [6–11]. The potential applications of host-guest macrocycle chemistry in recent years, especially for cucurbituril systems, have attracted much attention [10–15]. Complexes involving cucurbit[n]uril (CB[n]; $n = 5, 6, 7, 8, 10$) molecular container compounds have been studied in several conditions by many different techniques in both experimental and theoretical approaches [10–19].

The investigation of the electronic character of these systems has received special focus [16–19]. Buschmann and Zielesny propose a structural, electronic, and magnetic analysis of hemicucurbit[n]urils and its anionic complexes [20]. The authors conclude that hemicucurbit[n]urils with an odd number of imidazolidin-2-one units can easily be detected by the characteristic proton NMR absorption [20]. This technique has been used to analyze individual family of curcubit[n]uril in the isolated form, for example, Buschmann et al. show a detailed study of structure, electronic properties, and NMR-shielding of cucurbit[5]uril, decamethylcucurbit[5]uril, cucurbit[6]uril, cucurbit[7]uril, and cucurbit[8]uril [21].

Fileti and coauthors, using molecular dynamics (MD) and quantum chemical calculations (DFT and PM6 semi-empirical methods), present a structural analysis and complexion of the not-yet-synthesized cucurbit[9]uril (CB[9]) and fullerene C_{60} and show their potential for the creation of a new class of hosts

Electronic supplementary material The online version of this article (https://doi.org/10.1007/s00894-018-3719-3) contains supplementary material, which is available to authorized users.

✉ Guilherme Colherinhas
gcolherinhas@gmail.com

Eudes Eterno Fileti
fileti@gmail.com

Thaciana Malaspina
thacianavmf@gmail.com

[1] Departamento de Física - CEPAE and Instituto de Física, Universidade Federal de Goiás, Goiânia, GO 74690-900, Brazil

[2] Instituto de Ciência e Tecnologia, Universidade Federal de São Paulo, São José dos Campos, SP 12231-280, Brazil

for fullerene C_{60} [19]. This indicated a high structural compatibility between the two monomers (C_{60} and CB[9] exhibit virtually the same van der Waals radius), which is evident from the potential energy curve for the complexation process of the C_{60} into the CB[9] cavity. The potential energy curve demonstrated by the authors in this work shows two minimum points at 0.0 nm (full complexation) and about 0.6 nm (see the reference for more details). For the first time ref. [19] considered the C_{60} as an auxiliary guest in the CB[9] synthesis, the perfect fit of both nanosystems can lead to the formation of an unusual complex involving a carbon nanoparticle and a cucurbituril macrocycle. Experimental studies aiming at the detection of this complex certainly would benefit from complementary results to assist in its characterization. Then the computational determination of the magnetic signature of both host and guest molecules can be useful as a guide for experimental characterization of the C_{60}@CB[9] complexation.

In this work we extended the vision of the C_{60}@CB[9] system showing a detailed analysis of the magnetic shielding constant behavior for carbon, hydrogen, nitrogen, and oxygen atoms and the electronic structure of complex C_{60}@CB[9]. It is important to emphasize the effects due to the mutual interaction between the host and guest molecules on its magnetic signature in nonencapsulated and encapsulated states highlighting a persistent shielding of the molecules after separation. These data are important for the process of structural characterization when its synthesis is reached. We consider C_{60} and CB[9] monomers and the C_{60}@CB[9] complexes in the gas phase and in water solution using polarizable continuum model methodology and density functional theory.

Methods

The complexation involving the CB[9] cucurbituril and C_{60} fullerene, abbreviated herein as C_{60}@CB[9], consists of 222 atoms with a total of 1134 electrons. The energy-minimized structures of monomers and their complexes were obtained by the semi-empirical method, PM6, one of the most recent parametrizations of semi empirical methodology. Although semi empirical Hamiltonians may not perform perfectly for peculiar geometries, large excitations, and strongly nonequilibrated systems, they account for all quantum and many-body effects and have a relatively low computational cost when applied to large systems with satisfactory results providing an invaluable assistance in the preliminary screening of the condensed matter systems containing a significant number of electrons.

To characterize the complexation process of the C_{60} in the CB[9] cavity, a relaxed energy scan was performed. Thus, it was possible to obtain intermediate configurations by varying the distance between the center of mass (R_{CM}) of each monomers separated by 0.02 nm from $R_{CM} = 0.0$ nm (total complexation) to $R_{CM} = 0.9$ nm; Fig. 1 shows the monomers/complexes and the relative position between them. With these relaxed structures we calculate the values of the magnetic shielding constants for all carbon, hydrogen, nitrogen, and oxygen atoms using B3LYP hybrid functional (generalized gradient approximation) [22, 23], cc-pVDZ basis set functions, and gauge invariant atomic orbital approach (GIAO) [24, 25]. The GIAO-DFT approach offers a good compromise between computational cost and accuracy to determine the constant magnetic shielding [26–28]. The atomic charge was calculated using an electrostatic potential ChelpG method associated with B3LYP functional and cc-pVDZ and cc-pVTZ basis set functions. Solvent effects were included by employing the polarizable continuum model (PCM) [29, 30]. All quantum mechanics calculations were performed with the Gaussian 09 program [31].

Results

As demonstrated previously, C_{60} presents a high affinity for cucurbituril CB[9] because of the strong noncovalent collective interactions between the hydrophobic CB[9] internal cavity and the outer C_{60} surface [19]. This strong interaction is favored not only from the standpoint of energy but also the geometrical point of view and induces profound changes in the electron cloud of the fullerene. Thus, an expressive variation on the magnetic shielding constant inherently associated with a large variation in the dipole moment of the complex is expected. In this section, we will discuss the results for the nuclear magnetic shielding constant (σ) of the carbon atoms from C_{60} and for the carbon, oxygen, hydrogen, and nitrogen atoms from CB[9] both in isolated and complexed forms. For the complex forms, we show only results for the $R_{CM} = 0.0$, 0.2, 0.4, 0.6 and 0.9 nm.

Nuclear magnetic shielding constant

Fullerene C_{60} – $\sigma(^{13}C)$

Figure 2 show the analyses for nuclear shielding constant for each C_{60} carbon atom, both isolated (in red) and in C_{60}@CB[9] complex (in black) as a function of the center of mass distance of the monomers.

When inserted into a CB[9] cavity, the results for $\sigma(^{13}C)$'s fullerene atoms show considerable variation with a clear dependence of the distance between the center of mass of the compounds. For $R_{CM} = 0.0$ nm, we can observe that the $\sigma(^{13}C)$ is between 40 and 50 ppm with a larger number of atoms with spectroscopic signal in the ranges of 44–45 ppm and 46–47 ppm. This group of atoms with higher σ values is formed by carbon atoms near the ring of oxygen atoms that constitute the cavity of the CB[9]. For $R_{CM} = 0.2$ nm, $\sigma(^{13}C)$ practically stays between 40 and 51 ppm, with a larger number

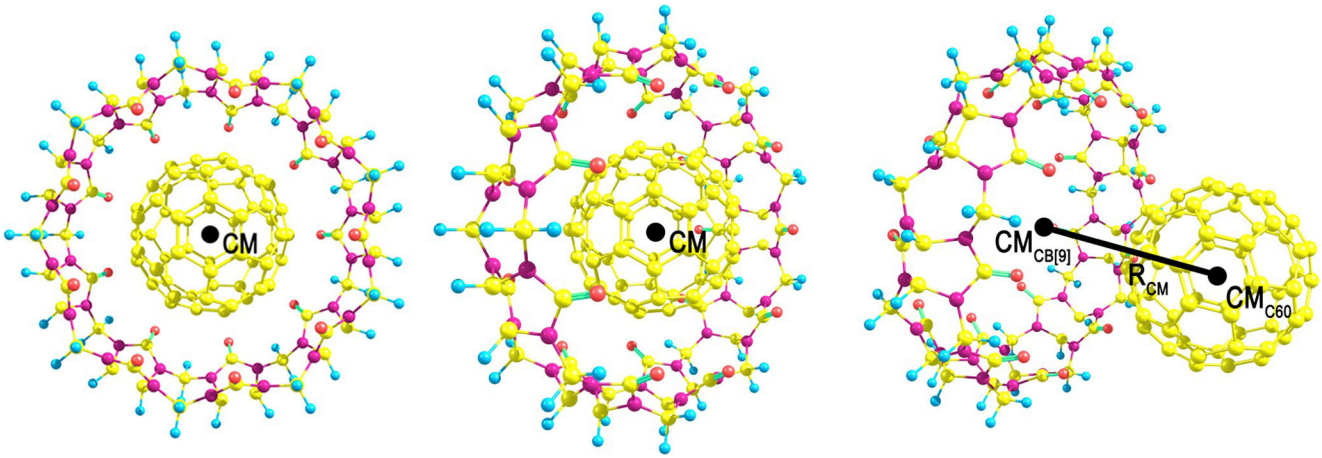

Fig. 1 C_{60} and CB[9] monomers/complexes center of mass (CM) and R_{CM} distance. In this work we use R_{CM} = 0.0, 0.2, 0.4, 0.6, and 0.9 nm

of atoms having a magnetic shield between 44 and 48 ppm. In this configuration C_{60} carbon atoms leave the CB[9] cavity, and therefore are subjected to a direct influence of the oxygen atoms of CB[9]. The values of $\sigma(^{13}C)$ for R_{CM} = 0.4 nm are similar to those obtained at 0.2 nm; however, their values are presented in the range of 38–52 ppm with most of the atoms presenting a constant shielding in the range of 44–48 ppm. From R_{CM} = 0.6 nm we observed a decrease in $\sigma(^{13}C)$ values, at R_{CM} = 0.6 nm a spectrum ranging from 39 to 48 ppm, and at R_{CM} = 0.9 nm the $\sigma(^{13}C)$ values are between 43 and 47 ppm. We note that with R_{CM} about 0.6 nm the C_{60} can be considered out of the cucurbituril monomer, and the intense influence of their oxygen atoms is no longer observed. From R_{CM} > 0.6 nm we can observe a slight reduction at the values fluctuation as can be seen in Fig. 2. This difference in the shielding constant behavior at 0.6 nm may be related to the interaction local minimum between the monomers as shown previously [19]. Overall we can see that at the complex all fullerene atoms are not shielded in comparison with the isolated corresponding. This is a consequence of the interaction of the C_{60} with the macrocycle that as shown earlier dramatically distorts its electron cloud [19]. We see that for all positions of R_{CM} high variation in magnetic shielding is found for all atoms, and even at a distance of 0.9 nm the C_{60} atoms remains unshielded. This residual not shielded after complex separation may be related to a charge transfer

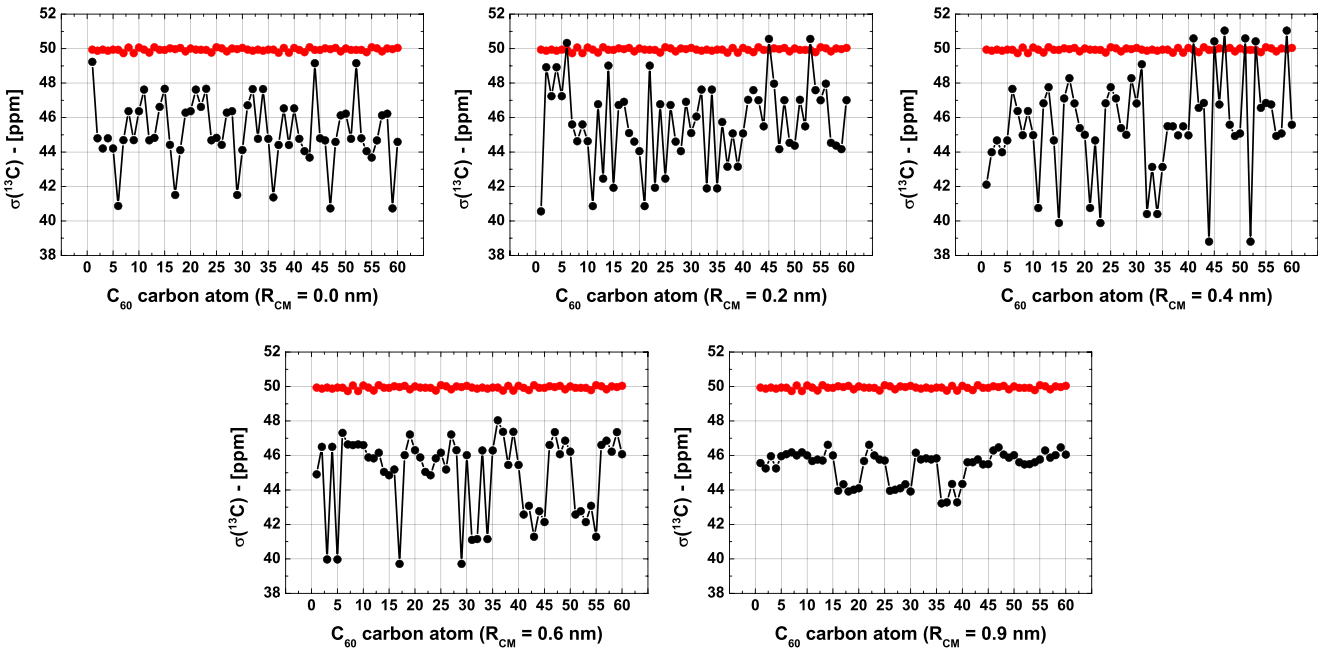

Fig. 2 Magnetic shielding constant $\sigma(^{13}C)$ for the fullerene atoms calculated at the B3LYP/cm^3-pVDZ level. Isolated C_{60} values are shown in red and C_{60}@CB[9] complex in black, for R_{CM} = 0.0, 0.2, 0.4, 0.6, and 0.9 nm

between the CB[9] and C_{60} and a discussion on this topic will be presented at the end of the text.

In an NMR experiment, the most accessible property is the chemical shift, which is obtained as the difference between the magnetic shielding of an isotope in different chemical environments, one of these being the standard reference environment [2, 32]. Here is the chemical shift as the difference $\delta(C) = \sigma(C)_{isol}^{CB[9]} - \sigma(C)_{R_{CM}}^{C_{60}@CB[9]}$. Figure 3 presents the chemical shift, $\delta(^{13}C)$, for two representative R_{CM} distances, 0.0 and 0.9 nm. The results show that $\delta(^{13}C)$ is between 1 and 9 ppm with an average of about 5 ppm at $R_{CM} = 0.0$ nm. At $R_{CM} = 0.9$ nm, the chemical shift ranges from 3.3 ppm to 4.2 ppm with an average of 4 ppm. Such values are expressive and clearly differ the isolated fullerene from its host complexed form. Also, it is interesting to note that even after the complex separation (at 0.9 nm) the shielding constants for some C_{60} atoms remain different from the corresponding isolated atoms C_{60}. In general, these differences favor shielding an experimental characterization of this compound by NMR techniques.

In aqueous solution, the $\sigma(^{13}C)$ results for the isolated fullerene differ in only 0.20 ppm of the results obtained in the gas phase. This is expected due to their hydrophobicity and low polarization. However, in the complex form the results obtained in water solution show a unique contribution of the solvent medium. This contribution is between −1.7 ppm and 1.2 ppm for $R_{CM} = 0.0$ nm and between −1.5 and 1.0 ppm for $R_{CM} = 0.9$ nm. These results do not change the conclusions obtained in the previous case, in the gas phase.

Cucurbituril CB[9] – $\sigma(^{13}C)$

The $\sigma(^{13}C)$ results for the isolated CB[9] compound were grouped into three levels of values near 47, 121, and 139 ppm (see Fig. 4), each level with 18 carbon atoms. As expected the magnetic shielding is related, among other factors, with the character of hybridization of the carbon. The first group consists of the sp^3 carbon atoms bonded to two nitrogen and two hydrogen atoms at the opening of the CB[9] macrocycle as shown in Fig. 5. Atoms in this neighborhood have a high magnetic shielding. The second group corresponds to equatorial carbon atoms at CB[9], having a neighborhood consisting of two nitrogen atoms, a hydrogen atom, and a carbon atom of the same group. This group features a magnetic shielding about 12% less than the former group. Finally, the third group comprises sp^2 carbon atoms bonded directly to the oxygen and nitrogen atoms. These groups are highly exposed to pairs of free electrons of other atoms and thus have a very low magnetic shielding.

The insertion of the C_{60} on CB[9] leads to a reduction of the shielding constant of all CB[9] carbon atoms. For the C_{60}@CB[9] at $R_{CM} = 0.0$ nm, we observe that the three characteristic groups of atoms show chemical shifts of about 5, 7, and 8 ppm, respectively, with $\sigma(^{13}C)$ values close of 42, 114, and 131 ppm. Nevertheless, the values relating to these reductions shows that, in percentage terms, the atoms of the first group are more magnetically sensitive than the other two groups (because of the way they are exposed), namely 11, 6, and 6%, respectively. We observed that the difference between the shielding constants does not show a strong dependence on the R_{CM} distance, i.e., its keeps approximately the same average value for any of the examined distances, as shown in Fig. 6.

Additionally, we can compare Figs. 3 and 6 to carbon atoms and ascertain that while the dispersion of the values for the chemical shift is greater for C_{60} in $R_{CM} = 0.0$ nm and lower in $R_{CM} = 0.9$ nm, the opposite occurs for the CB[9] for which a greater dispersion of values is observed in $R_{CM} = 0.9$ nm. This is due to the greater structural distortion suffered by C_{60} inside the macrocycle. As expected, the influence of the solvent effects for the constant magnetic shielding for the CB[9] carbon atoms is small. Once isolated, the solution results differ between −0.8 ppm and 2.5 ppm of the results obtained in the gas phase. This variation is virtually maintained even in the presence of the C_{60}. For $R_{CM} = 0.0$ nm

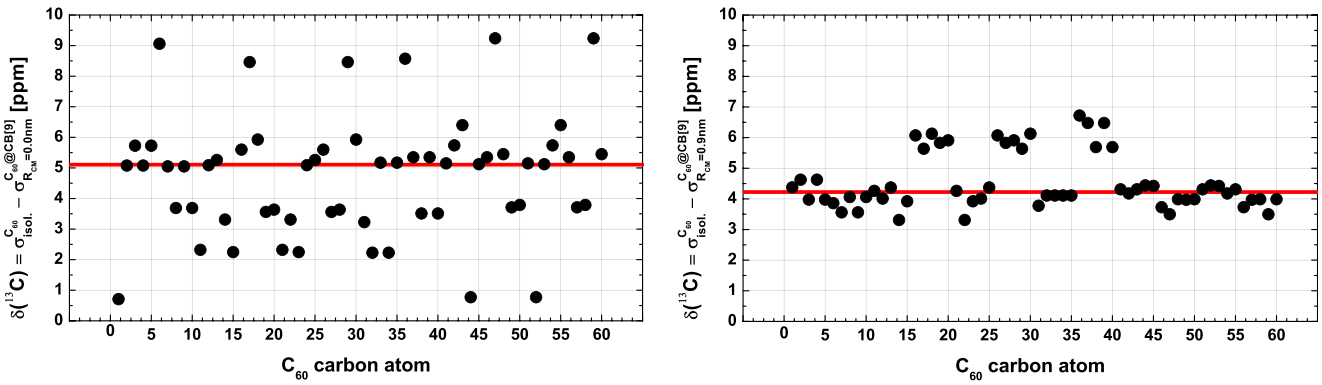

Fig. 3 Analysis of the variation range of the chemical shift of fullerene C_{60} carbon atoms for $R_{CM} = 0.0$ nm (left) and 0.9 nm (right). The horizontal red line represents the average

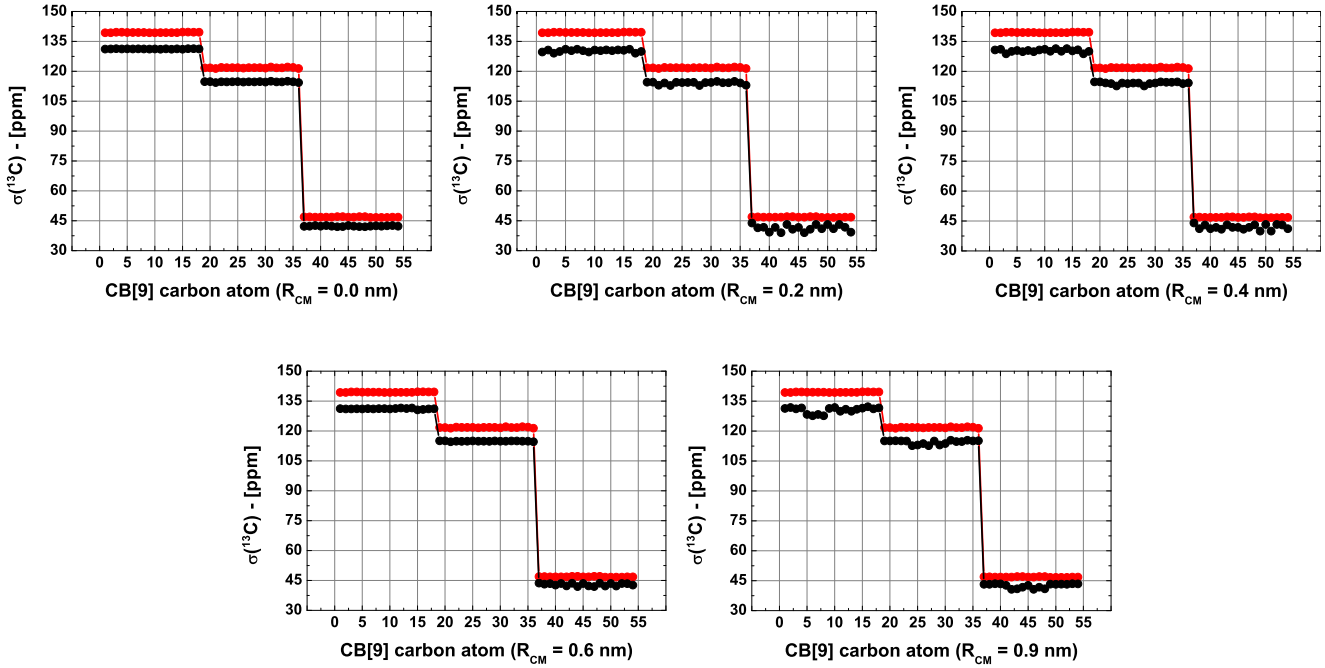

Fig. 4 Magnetic shielding constant $\sigma(^{13}C)$ for the CB[9] carbon atoms calculated in B3LYP/cm^3-pVDZ level. Isolated CB[9] values are shown in red and C_{60}@CB[9] complex in black, for R_{CM} = 0.0, 0.2, 0.4, 0.6, and 0.9 nm

[R_{CM} = 0.9 nm] we observed a solvent effect between −0.6 to 2.9 ppm [−0.8 to 3.4 ppm] for constant magnetic shielding.

Cucurbituril CB[9] – $\sigma(^{17}O)$

The results for the constant magnetic shielding of the CB[9] oxygen atoms, $\sigma(^{17}O)$, are shown in Fig. S1. These results confirm that $\sigma(^{17}O)$ values are almost constant when obtained for the isolated CB[9], close to 57 ppm, which indicates that oxygen atoms are exposed essentially to the same chemical environment. For the oxygen at complexed CB[9], the shielding constant values obey the same tendency (see Fig. S1). The interaction of the fullerene C_{60} results in a strong reduction of the magnetic shielding constant of the oxygen atoms. This change in magnetic signature of oxygen atoms is provided by modifying the electron density of the CB[9] that interacts with the electron density of the C_{60} fullerene. In this condition, $\sigma(^{17}O)$ values are shown between 30 and 40 ppm, 20 and 40 ppm, 20 and 35 ppm, 25 and 35 ppm, and 20 and 40 ppm, respectively for R_{CM} = 0.0 nm, 0.2 nm, 0.4 nm, 0.6 nm, and 0.9 nm. Overall this corresponds to a chemical shift of about 25 ppm for any oxygen atom, as can be seen in Fig. 6, independent of the distance between the monomers. This expressive reduction in magnetic signature demonstrates the strong interaction between the oxygen atoms and the C_{60} π electrons. The results show that in both cases — CB[9] oxygen atoms and C_{60} carbon atoms — we observe significant modifications in the σ values possibly due to the modification of the electronic structure of the two molecules and existing even when the molecules are separated by almost 1 nm.

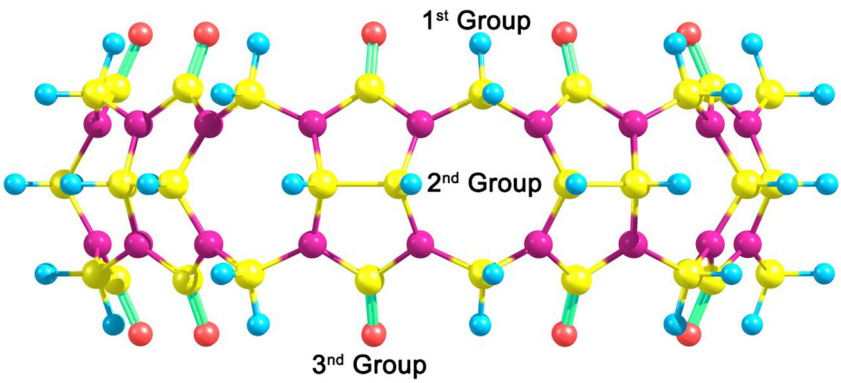

Fig. 5 Identification of carbon atom groups in the CB[9]. Carbon, hydrogen, nitrogen, and oxygen are represented in yellow, blue, purple, and red, respectively

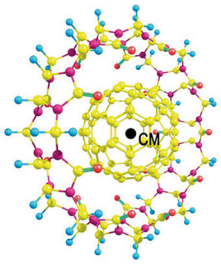

R_{CM} = 0.0 nm

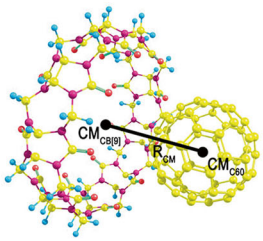

R_{CM} = 0.9 nm

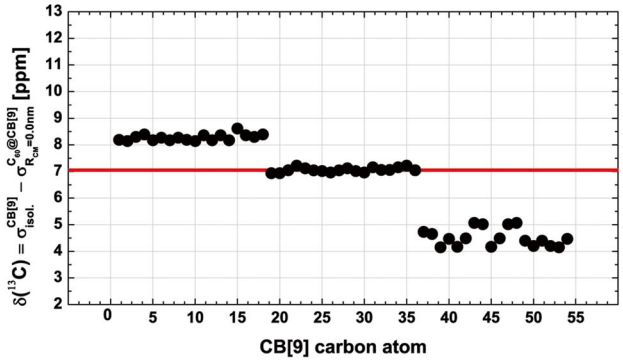

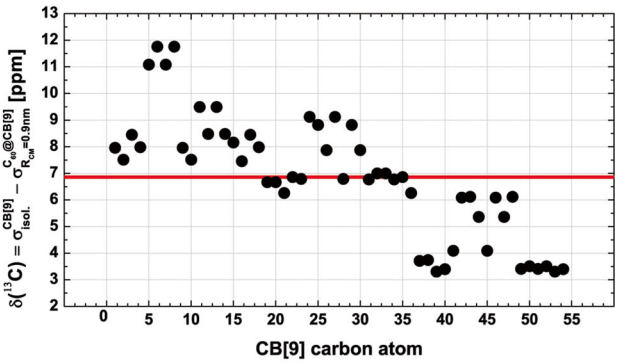

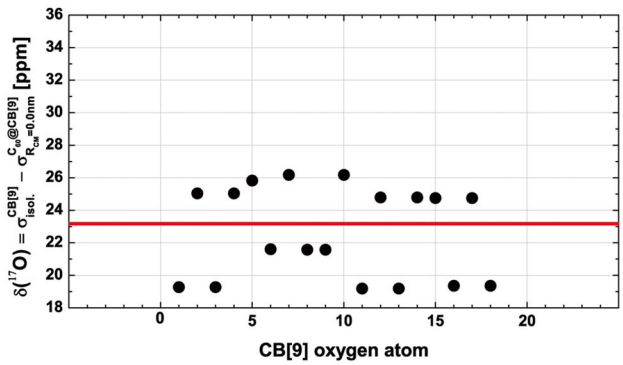

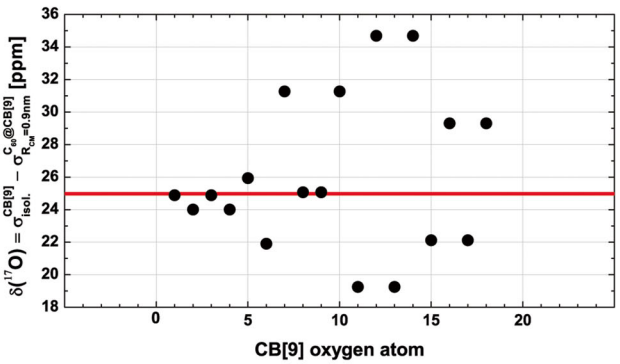

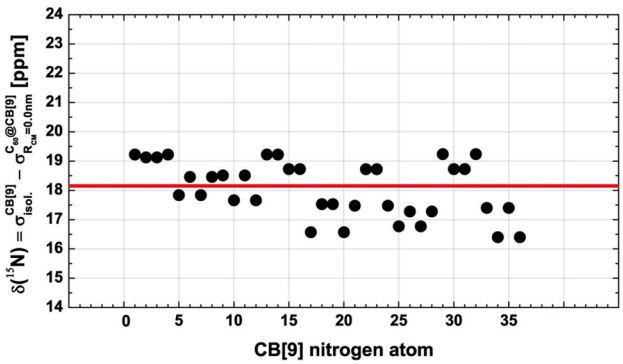

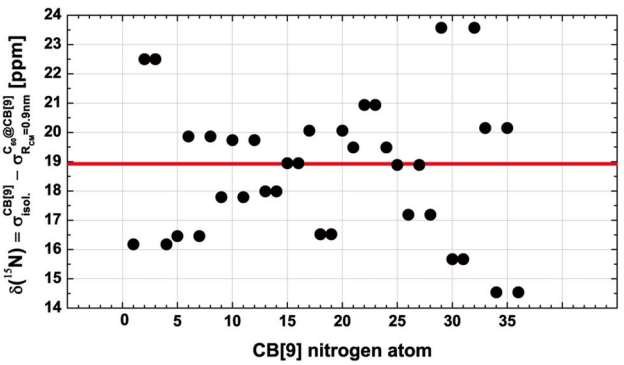

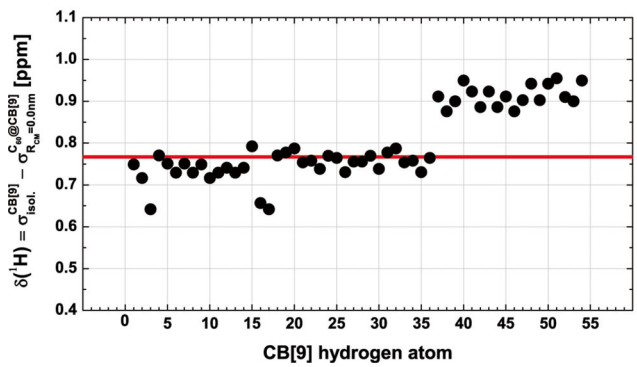

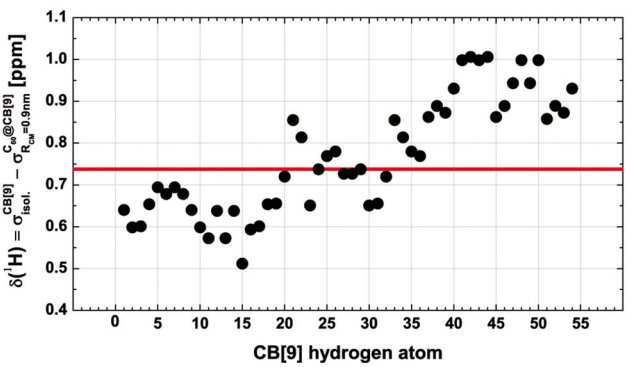

◀ **Fig. 6** Analysis of the variation range of the chemical shift of the CB[9] atoms for $R_{CM} = 0.0$ nm and 0.9 nm. The horizontal red line represents the average

In general, the magnetic properties of the oxygen atoms are greatly influenced by the solvent effects. The results for the magnetic shielding constant of the isolated CB[9] in aqueous solution is approximately 30 ppm higher than that obtained in the gas phase, proving to be more shielded. However, in the complex form C_{60}@CB[9], the CB[9] oxygen atoms are slightly less exposed to the solvent. For $R_{CM} = 0.0$ nm [$R_{CM} = 0.9$ nm], $\sigma(^{17}O)$ values show a difference with the complex C_{60}@CB[9] gas phase results between 24 and 26 ppm [28 and 31 ppm], proving to be more shielded in water solution. We note that during the removal of C_{60} of the complex, the shielding constant of CB[9] oxygen atoms show a similar behavior to that obtained when in the gas phase.

Cucurbituril CB[9] – $\sigma(^{15}N)$

For gas phase isolated CB[9], the results for $\sigma(^{15}N)$ indicate an average value over all atoms of around 150 ppm (see Fig. S2). The insertion of C_{60} ($R_{CM} = 0.0$ nm) reduces the $\sigma(^{15}N)$ values at approximately 20 ppm. Although intense, these chemical shifts are less than those observed for the oxygen atoms. The removal of the fullerene C_{60} ($R_{CM} > 0.0$ nm) results in $\sigma(^{15}N)$ values ranging from 125 to 135 ppm. For this case, the $\delta(^{15}N)$ values are between 15 and 24 ppm, as shown in Fig. 6. The solvent effects for the magnetic shielding constant of nitrogen atoms are relatively small for this system. For CB[9] isolated, the solvent effects reduce the shielding constant at about 2 ppm, when compared with gas phase results. In the complex C_{60}@CB[9] form the results for $R_{CM} = 0.0$ nm [$R_{CM} = 0.9$ nm] are between 2 and 3 ppm [1 and 3 ppm].

Cucurbituril CB[9] – $\sigma(^{1}H)$

In general, the behavior of the $\sigma(^{1}H)$ values is very similar to the $\sigma(^{13}C)$, and three different groups for the values for $\sigma(^{1}H)$ were also observed. The first group shows a value close to 25.5 ppm, the second group around 27.5 ppm, and the third group around 28.5 ppm (as shown in Fig. S3), with each group containing 18 hydrogen atoms, and Fig. 7 show these groups in CB[9]. The presence of fullerene C_{60} reduces these values at approximately between 0.7 to 1.3 ppm, resulting a $\delta(^{1}H)$ average of 0.9 ppm as shown in Fig. 6. This chemical shift, though small, is easily detectable in NMR experiments. In general, the solvent effects for hydrogen magnetic shielding constants of the CB[9] are between −0.5 to 0.5 ppm independent of the presence of the fullerene C_{60}.

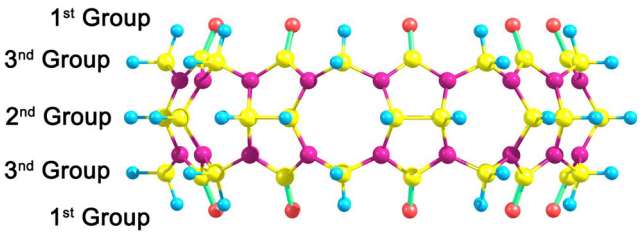

Fig. 7 Identification of hydrogen atom groups in the CB[9]. Carbon, hydrogen, nitrogen, and oxygen are represented in yellow, blue, purple, and red, respectively

Atomic charge

We conjecture that the remaining shielding on the C_{60} carbon atoms after complete separation of the complex is due to a charge transfer between the monomeric species. To investigate this possibility, we perform population analysis of ChelpG in B3LYP/cm^3-pVDZ theoretical level calculations. This analysis shows considerable charge transfer between the monomers C_{60} and CB[9], indicating that approximately 0.517e is transferred from the C_{60} to the CB[9] when encapsulated (configuration for $R_{CM} = 0.0$ nm). After the separation process was observed, the amount of charge on C_{60} decreases to approximately 0.249e at $R_{CM} = 0.9$ nm. More sophisticated calculations, using the cc-pVTZ basis set, confirm the same trends. For configuration $R_{CM} = 0.9$ nm, we observed a charge transfer with approximately 0.296e (cc-pVTZ). This charge transfer was also observed for the system in aqueous solution. The B3LYP/cm^3-pVDZ [B3LYP/cm^3-pVTZ] results for $R_{CM} = 0.0$ nm are equal to 0.462e and for $R_{CM} = 0.9$ nm are equal to 0.293e [0.372e]. Considering the sensitivity of the C_{60} electronic cloud to any change in its chemical environment, we believe that the residual shielding on the carbon atoms over long distances is due exclusively to this charge transfer between the two monomers. Figure 8 (left panel) shows the evolution of the results of ChelpG B3LYP/cm^3-pVDZ for q values of each monomer relative to the distance of the center of mass of the monomers for gas phase settings. Figure 8 (right panel) shows a comparison between the profile of the magnetic shielding constant of the carbon atoms and the Mulliken atomic charge of these atoms for the CB[9] and C_{60} monomers, $R_{CM} = 0.9$ nm. We can observe that the $\sigma(^{13}C)$ profile has similar separation to the charge distribution profile on the atoms for CB[9], as already observed in previous works [05]. For the C_{60}, despite difficult visual separation, we can see that less shielded atoms have a higher charge value compared to the more shielded atoms. Similar results were observed for the other R_{CM} calculations and atoms. The values for the Mulliken atomic charge were obtained from the same calculation of the shielding constant, and therefore

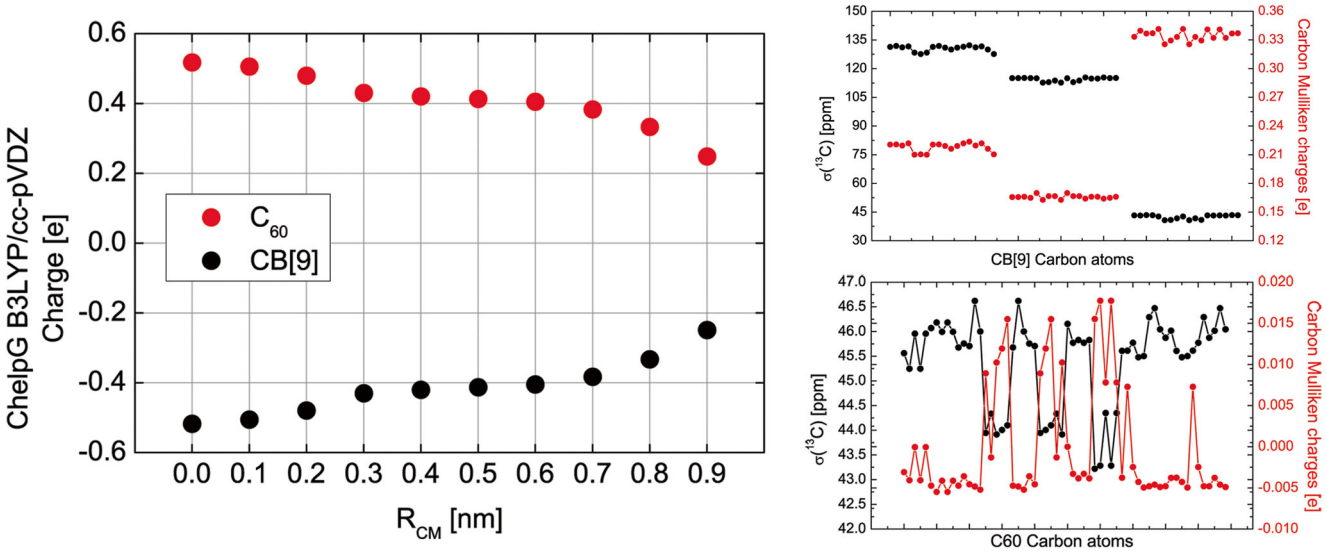

Fig. 8 (Left) Evolution of the ChelpG B3LYP/cm^3-pVDZ charges of the monomers relative to the distance of the center of mass R_{CM} (gas phase setting); (Right) profile of the GIAO-B3LYP/cm^3-pVDZ magnetic shielding constant for carbon atoms and the carbon Mulliken atomic charge for CB[9] and C_{60} for $R_{CM} = 0.9$

reflect a real influence of the electronic density on the values of the magnetic shielding constant.

Conclusions

DFT calculations were performed at the B3LYP/cm^3-pVDZ theoretical level, using the gauge invariant atomic orbital approach to describe the magnetic shielding constants and chemical shifts for all atoms in the C_{60}@CB[9] host-guest complex. The chemical shift between atoms in the complex and their corresponding isolated monomers was calculated for all isotopes. For the C_{60} carbon atoms, we observe that the magnetic shielding is in the range from 40 to 50 ppm, depending on the site where the carbon atom is located in the cage. Chemical shifts due to complexation were found to be 5 ppm at R_{CM} = 0.0 nm and 4 ppm at $R_{CM} = 0.9$ nm and not to depend significantly on the separation distance between the centers of mass of the monomers. Residual shielding observed for C_{60} after the separation of the complex can be attributed to the charge transfer that occurs during the interaction process. Our population analysis indicated that a charge of +0.296e and + 0.372e was transferred to the C_{60} for gas phase and water solution systems, respectively.

The results for the atoms of CB[9] also indicate significant chemical shifts. The chemical shift for the carbon atoms ranges from 5 to 8 ppm depending on their position in the macrocycle. For the oxygen atom the chemical shift is higher, reaching an average value of 33.5 ppm. The nitrogen atom presented a chemical shift between 18 and 24 ppm, while for hydrogen deviations it was around 1 ppm. These values describe the effects of the mutual interaction between monomers in the complex on the magnetic shielding of their atoms. This study therefore quantifies the magnitude of the mutual induced chemical shifts in this host-guest system, which can be useful for future characterization and evidence of the encapsulation of the fullerene C_{60} by the cucurbituril CB[9] by NMR experiments.

Acknowledgments This work was supported by grants from Brazilian agencies FAPEG, FAPESP, and CNPq.

References

1. Zalesskiy SS, Danieli E, Blumich B, Ananikov VP (2014) Miniaturization of NMR systems: desktop spectrometers, microcoil spectroscopy, and "NMR on a Chip" for chemistry, biochemistry, and industry. Chem Rev 114:5641–5694
2. Toukach FV, Ananikov VP (2013) Recent advances in computational predictions of NMR parameters for the structure elucidation of carbohydrates: methods and limitations. Chem Soc Rev 42: 8376–8415
3. Gancheff JS, Denis PA (2015) Relative affinity of bambus[6]uril towards halide ions: a DFT/GIAO approach in the gas phase, and in the presence of the solvent employing discrete and discrete-continuum models. Comput Theor Chem 1064:35–44
4. Colherinhas G, Fonseca TL, Georg HC, Castro MA (2011) Isomerization effects on chemical shifts and spin-spin coupling constants of polyacetylene chains: a GIAO-DFT study. Int J Quantum Chem 111:1616–1625
5. Colherinhas G, Fonseca TL, Castro MA (2011) ^{13}C chemical shifts of polyacetylene chains with charged conformational defects: a GIAO–DFT study. Chem Phys Lett 503:191–196
6. Simoes SM, Rey-Rico A, Concheiro A, Alvarez-Lorenzo C (2015) Supramolecular cyclodextrin-based drug nanocarriers. Chem Commun (Camb) 51:6275–6289
7. Kang Y, Guo K, Li BJ, Zhang S (2014) Nanoassemblies driven by cyclodextrin-based inclusion complexation. Chem Commun (Camb) 50:11083–11092

8. Nimse SB, Kim T (2013) Biological applications of functionalized calixarenes. Chem Soc Rev 42:366–386
9. Zadmard R, Alavijeh NS (2014) Protein surface recognition by calixarenes. RSC Adv 4:41529–41542
10. Assaf KI, Nau WM (2015) Cucurbiturils: from synthesis to high-affinity binding and catalysis. Chem Soc Rev 44:394–418
11. Masson E, Ling X, Joseph R, Kyeremeh-Mensah L, Lu X (2012) Cucurbituril chemistry: a tale of supramolecular success. RSC Adv 2:1213–1247
12. Zhao W, Wang C, Zhang Y, Xue S, Zhu Q, Tao Z (2015) Supramolecular assembly of a methyl-substituted cucurbit[6]uril and its potential applications in selective sorptio. New J Chem 39:2433–2436
13. Kubota R, Hamachi I (2015) Protein recognition using synthetic small-molecular binders toward optical protein sensing in vitro and in live cells. Chem Soc Rev 44:4454–4471
14. Ghale G, Nau WM (2014) Dynamically analyte-responsive macrocyclic host–fluorophore systems. Acc Chem Res 47:2150–2159
15. Yang H, Yuan B, Zhang X, Scherman OA (2014) Supramolecular chemistry at interfaces: host-guest interactions for fabricating multifunctional biointerfaces. Acc Chem Res 47:2106–2015
16. Pinjari RV, Gejji SP (2008) Electronic structure, molecular electrostatic potential, and NMR chemical shifts in cucurbit[n]urils (n = 5-8), ferrocene, and their complexes. J Phys Chem A 112:12679–12686
17. Gobre VV, Pinjari RV, Gejji SP (2010) Density functional investigations on the charge distribution, vibrational spectra, and NMR chemical shifts in cucurbit[n]uril (n = 5-12) hosts. J Phys Chem A 114:4464–4470
18. Barooah N, Sundararajan M, Mohanty J, Bhasikuttan AC (2014) Synergistic effect of intramolecular charge transfer toward supramolecular pKa shift in cucurbit[7]uril encapsulated coumarin dyes. J Phys Chem B 118:7136–7146
19. Fileti E, Colherinhas G, Malaspina T (2014) Predicting the properties of a new class of host–guest complexes: C60 fullerene and CB[9] cucurbituril. Phys Chem Chem Phys 16:22823–22829
20. Buschmann HJ, Zielesny A (2013) Geometric, electronic and NMR properties of hemicucurbit[n]urils and their anionic complexes. Comput Theor Chem 1022:14–22
21. Buschmann HJ, Wego A, Zielesny A, Schollmeyer E (2006) Structure, electronic properties and NMR-shielding of cucurbit[n]urils. J Incl Phenom Macrocycl Chem 54:85–88
22. Becke AD (1993) Density-functional thermochemistry. III. The role of exact exchange. J Chem Phys 98:5648
23. Lee C, Yang W, Parr RG (1988) Development of the Colle-Salvetti correlation-energy formula into a functional of the electron density. Phys Rev B 37:785
24. Ditchfield R (1974) Self-consistent perturbation theory of diamagnetism. Mol Phys 27:789–807
25. Wolinski K, Hinton JF, Pulay P (1990) Efficient implementation of the gauge-independent atomic orbital method for NMR chemical shift calculations. J Am Chem Soc 112:8251–8260
26. Pascual-Borras M, Lopez X, Poblet JM (2015) Accurate calculation of (31)P NMR chemical shifts in polyoxometalates. Phys Chem Chem Phys 17:8723–8731
27. Gerber IC, Jolibois F (2015) Theoretical gas to liquid shift of (15)N isotropic nuclear magnetic shielding in nitromethane using ab initio molecular dynamics and GIAO/GIPAW calculations. Phys Chem Chem Phys 17:12222–12227
28. Vahakangas J, Ikalainen S, Lantto P, Vaara J (2013) Nuclear magnetic resonance predictions for graphenes: concentric finite models and extrapolation to large systems. Phys Chem Chem Phys 15:4634–4641
29. Tomasi J, Mennucci B, Cammi R (2005) Quantum mechanical continuum solvation models. Chem Rev 105:2999–3094
30. Miertuš S, Scrocco E, Tomasi J (1981) Electrostatic interaction of a solute with a continuum. A direct utilizaion of AB initio molecular potentials for the prevision of solvent effects. Chem Phys 55:117–129
31. Frisch MJ et al (2009) Gaussian 09. Gaussian, Inc., Wallingford
32. Mulder FA, Filatov M (2010) NMR chemical shift data and ab initio shielding calculations: emerging tools for protein structure determination. Chem Soc Rev 39:578–590